RECENT HARD PROBE MEASUREMENTS WITH STAR AT RHIC*

Jana Bielčíková

for the STAR Collaboration

Nuclear Physics Institute of the Czech Academy of Sciences
250 68 Řež, Czech Republic

(Received October 9, 2019)

Hot and dense QCD matter created in high-energy heavy-ion collisions at the Relativistic Heavy Ion Collider (RHIC) manifests properties of strongly coupled liquid with very low viscosity. High statistics data and major upgrades of the STAR experiment started a new era of tomography of the QCD matter at RHIC using hard probes. In particular, the Heavy Flavor Tracker (HFT) enables precision measurements of open heavy-flavor hadrons and the Muon Telescope Detector (MTD) greatly improves quarkonium measurements. These studies are complemented by measurements of jet properties that provide further insights into the partonic energy loss in the QCD matter. In these proceedings, an overview of recent results on open heavy-flavor hadron, quarkonium, and jet production in Au+Au collisions at the top RHIC collision energy $\sqrt{s_{NN}} = 200$ GeV in the center of mass per nucleon–nucleon pair measured with STAR is presented.

DOI:10.5506/APhysPolBSupp.13.109

1. Production of open-charm hadrons

In high-energy heavy-ion collisions, heavy-flavor (c and b) quarks are primarily produced in initial hard parton scatterings and are ideally suited for studies of the quark–gluon plasma (QGP) properties. Measurements of charm hadron nuclear modification factor R_{AA}, which is the ratio of charm hadron spectra in $A+A$ to that in $p+p$ collisions scaled by the number of binary collisions, provide insights into the parton energy loss mechanism. Taking advantage of the high statistics data from 2014 with the high precision HFT, the R_{AA} for D^0 mesons was measured down to low transverse momentum (p_{T}) [1] as shown in figure 1 (left). The D^0-meson production in central Au+Au collisions is strongly suppressed relative to that in $p+p$

* Presented at "Excited QCD 2019", Schladming, Austria, January 30–February 3, 2019.

collisions. This finding is complemented by the measurement with $D^{\pm}$ mesons which show the same level of suppression. The D-meson suppression is similar to light flavor hadrons and challenges models of the flavor dependence of parton energy loss. Figure 1 (right) presents the elliptic flow (v_2) of D^0 mesons scaled by the number of constituent quarks (n_q) as a function of n_q-scaled transverse kinetic energy ($m_{\mathrm{T}} - m_0$). The n_q-scaled v_2 results for D^0 mesons are compatible with those of light flavor hadrons suggesting that the c quarks exhibit the same collective behavior as light flavor quarks.

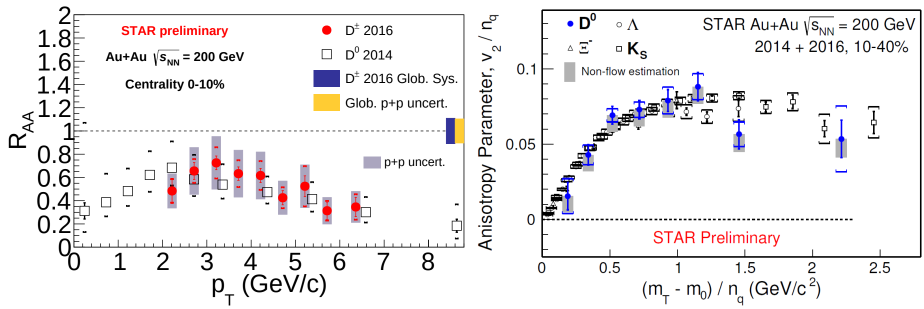

Fig. 1. R_{AA} of D^0 [1] and $D^{\pm}$ mesons in central Au+Au collisions at $\sqrt{s_{NN}} = 200$ GeV (left). The elliptic flow scaled by the number of constituent quarks (v_2/n_q) for D^0 mesons compared to other hadrons (right) in semi-central Au+Au collisions.

The hadronization of c quarks can be studied through the ratios of yields of charm hadrons, in particular, the $\Lambda_c^{\pm}/D^0$ ratio. If c quarks hadronize via the coalescence, an enhancement of this ratio relative to $p+p$ collisions is expected at the intermediate $p_{\mathrm{T}} = 2$–6 GeV$/c$. Figure 2 shows the p_{T} and collision centrality dependence of the $\Lambda_c^{\pm}/D^0$ ratio in Au+Au collisions.

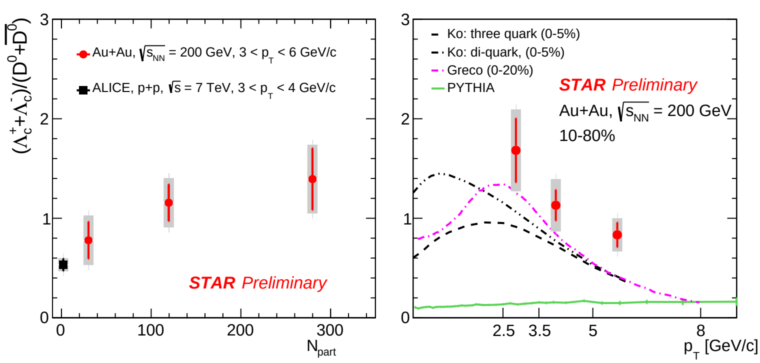

Fig. 2. The $\Lambda_c^{\pm}/D^0$ ratio as a function of p_{T} in 10–80% centrality (left) and as a function of N_{part} for $3 < p_{\mathrm{T}} < 6$ GeV$/c$ (right) in Au+Au collisions at $\sqrt{s_{NN}} = 200$ GeV.

There is a significant enhancement of this ratio compared to the $p+p$ reference and the enhancement increases with centrality. The SHM model [2] underpredicts the measured ratio, while the calculations including coalescence of thermalized charm quarks [3, 4] are closer to the data.

Combining the D^0, $D^{\pm}$, Λ_c measurements with the $D_s^{\pm}$ [5], the $c\bar{c}$ production cross section per binary nucleon collision in Au+Au collisions was extracted and is consistent with that in $p+p$ collisions. The observed suppression of D-meson yields is compensated by the enhanced Λ_c production suggesting significant modifications to charm quark hadronization and hadrochemistry in the presence of the QGP.

2. Production of bottomonia

In the past, suppression of J/ψ (charmonium) production due to the color-screening effect was proposed as a key signature of the QGP formation [6]. However, other competing effects such as cold nuclear matter (CNM) effects and regeneration influence the J/ψ production as well. Therefore, the focus of experimental studies shifted to measurements of Υ (bottomonium) production for which these effects play a smaller role. Moreover, different binding energies of the bottomonium states lead to their temperature-dependent dissociation and this 'sequential suppression' can help to constrain the temperature of the medium created in heavy-ion collisions.

Figure 3 shows the centrality dependence of R_{AA} of $\Upsilon(1S)$ and $\Upsilon(2S+3S)$ states in Au+Au collisions at mid-rapidity. To increase the precision of the measurement, results from both the e^+e^- decay channel using electromagnetic calorimeter triggered data from 2011 and the $\mu^+\mu^-$ channel using the MTD triggered data from 2014 and 2016 were combined. The data demonstrate a clear suppression of the bottomonium production which increases from peripheral to central Au+Au collisions and is stronger for the excited Υ states, consistent with the sequential suppression scenario of quarkonia in QGP. The data are compared with two theoretical calculations. The calculation labeled 'Rothkopf' [7] uses a lattice-vetted heavy-quark potential embedded in a hydrodynamically evolving medium without inclusion of the CNM effects or regeneration. The calculation describes well the measured R_{AA} for the $\Upsilon(1S)$ state but underestimates the suppression of the excited states in peripheral Au+Au collisions. The second calculation labeled 'Rapp' [8] is based on a kinetic rate equation and temperature-dependent binding energies and, in contrast to the previous calculation, it includes the regeneration and CNM effects. This model calculation is able to qualitatively describe the measured R_{AA} for both the ground and excited bottomonia states. It is interesting to note that the ground state suppression is similar to that measured by CMS at the LHC at $\sqrt{s_{NN}} = 2.76$ TeV [9], but the STAR data indicate a smaller suppression of the excited states.

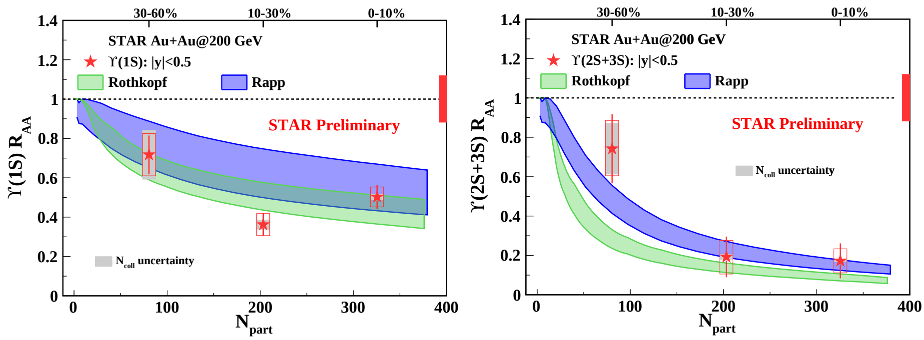

Fig. 3. R_{AA} of $\Upsilon(1S)$ (left) and $\Upsilon(2S+3S)$ (right) states as a function of centrality in Au+Au collisions at $\sqrt{s_{NN}} = 200$ GeV. The data are compared to model calculations from [7] and [8].

3. Production of jets

Next, we discuss the STAR results on jet production and its modification in central Au+Au collisions. Semi-inclusive distributions of jets recoiling from a high-p_{T} hadron were recently used to explore jet quenching [10]. A strong suppression of the yields for jet radii $R = 0.2$–0.5 using a low p_{T}-cutoff ($p_{\mathrm{T}} > 0.2$ GeV/c) on jet constituents was measured. This corresponds to medium-induced energy transport to large angles relative to the jet axis of 3–5 GeV/c, smaller than that measured at the LHC energy [11]. Within uncertainties, no evidence for intra-jet broadening within an angle of 0.5 relative to the jet axis was observed. New measurements using direct photon (γ_{dir}) or neutral pion (π^0) produced in coincidence with a recoiling charged jet are presented here and provide further insight into the dependence of energy loss on the color factor, path length, and the initial parton energy. The suppression of the recoil-jet per-trigger yield in Au+Au collisions is quantified by calculating the yield ratio in Au+Au relative to that in $p+p$ (I_{AA}). As the $p+p$ measurement is not available for γ triggers, PYTHIA validated on π^0+jet data is used instead. Figure 4 compares I_{AA}^{PYTHIA} for π^0+jet and γ_{dir}+jet. A strong suppression of the yields is observed with a similar level of suppression for both trigger types without any clear $E_{\mathrm{T}}^{\mathrm{trig}}$ dependence. Comparison of π^0+jet with previously published hadron+jet results [10] shows that π^0+jet and hadron+jet have a similar level suppression. More differential studies including the azimuthal distributions of recoiling jets that are expected to be sensitive to quasiparticle nature of the medium in the tail of the distribution are ongoing.

STAR also performed a measurement of di-jet transverse momentum asymmetry (A_J) [12]. To minimize the effects of the background fluctuations and combinatorial jets, di-jets were first reconstructed with constituents with

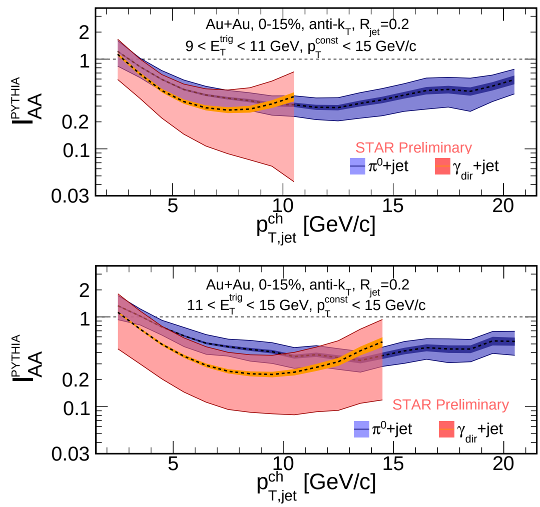

Fig. 4. (Color online) $I_{AA}^{\rm PYTHIA}$for $\gamma_{\rm dir}$- (light gray/red) and π^0-trigger (dark gray/blue) recoil charged jets with $9 < E_{\rm T}^{\rm trig} < 11$ GeV (left) and $11 < E_{\rm T}^{\rm trig} < 15$ GeV (right) in Au+Au collisions at $\sqrt{s_{NN}} = 200$ GeV. Lighter (darker) bands represent syst. (stat.) uncertainties.

$p_{\rm T} > 2$ GeV$/c$ reffered to as HardCore jets. The two highest-energy back-to-back HardCore jets were found to display a significantly stronger momentum imbalance in Au+Au collisions than in the $p+p$ data. Including soft particles with $p_{\rm T} > 0.2$ GeV$/c$ to jets and performing geometrical matching with the HardCore jets within $\Delta R < 0.4$, the di-jet momentum balance for such 'Matched' jets is restored for the jet resolution parameter $R = 0.4$, while for $R = 0.2$, significant remaining momentum imbalance relative to $p+p$ reference persists. This indicates that the energy lost by a parton in the medium re-emerges as soft constituents accompanied with a small, but significant, broadening of the jet structure compared to $p+p$. The jet–medium interaction could further depend on the resolution scale or the coherence length of the medium which then sees the jet either as a single object or a multi-prong object. Here, we discuss the A_J dependence on the angular scale. Figure 5 shows the A_J for HardCore and Matched recoil jets for two selections of the angle between the leading and sub-leading sub-jets ($\theta_{\rm SJ}$): inclusive $\theta_{\rm SJ} = (0.1, 0.4)$ (black circles) and wide $\theta_{\rm SJ} = (0.2, 0.3)$ (red diamonds), respectively. The HardCore jets demonstrate a di-jet imbalance also for wide angles. On the other hand, the Matched jets are balanced for both $\theta_{\rm SJ}$ selections, consistent with the previous measurement. Further differential analyses to extract the medium resolution scale or the coherence length using new high statistics data from STAR are ongoing.

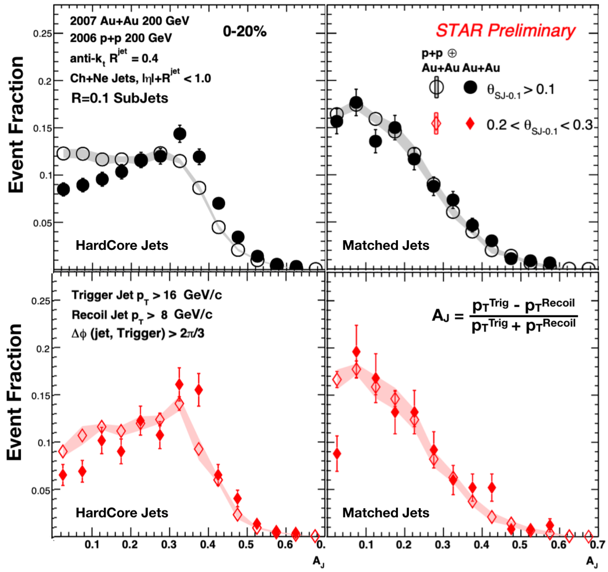

Fig. 5. (Color online) HardCore and Matched di-jet asymmetry ($|A_J|$). See the text for details on marker description.

This work was supported by the ESF grant CZ.02.1.01/0.0/0.0/16_013/0001569 of the Ministry of Education, Youth and Sports of the Czech Republic.

REFERENCES

[1] J. Adam *et al.* [STAR Collaboration], *Phys. Rev. C* **99**, 034908 (2019).

[2] I. Kuznetsova, J. Rafelski, *Eur. Phys. J. C* **51**, 113 (2007).

[3] S. Ghosh *et al.*, *Phys. Rev. D* **90**, 054018 (2014).

[4] S.H. Lee *et al.*, *Phys. Rev. Lett.* **100**, 222301 (2008).

[5] L. Zhou [STAR Collaboration], *Nucl. Part. Phys. Proc.* **289–290**, 241 (2017).

[6] T. Matsui, H. Satz, *Phys. Lett. B* **178**, 416 (1986).

[7] B. Krouppa, A. Rothkopf, M. Strickland, *Phys. Rev. D* **97**, 016017 (2018).

[8] X. Du, R. Rapp, M. He, *Phys. Rev. C* **96**, 054901 (2017).

[9] V. Khachatryan *et al.* [CMS Collaboration], *Phys. Lett. B* **770**, 357 (2017).

[10] L. Adamczyk *et al.* [STAR Collaboration], *Phys. Rev. C* **96**, 024905 (2017).

[11] J. Adam *et al.* [ALICE Collaboration], *J. High Energy Phys.* **1509**, 170 (2015).

[12] L. Adamczyk *et al.* [STAR Collaboration], *Phys. Rev. Lett.* **119**, 062301 (2017).